Journal of Experimental Botany, Vol. 69, No. 22 pp. 5477–5488, 2018
doi:10.1093/jxb/ery315 Advance Access publication 19 September 2018

RESEARCH PAPER

Enhanced Rubisco activation associated with maintenance of electron transport alleviates inhibition of photosynthesis under low nitrogen conditions in winter wheat seedlings

Jingwen Gao[1,*], Feng Wang[2,*], Jianyun Sun[3,*], Zhongwei Tian[1], Hang Hu[1], Suyu Jiang[1], Qiuci Luo[1], Yun Xu[1], Dong Jiang[1], Weixing Cao[1] and Tingbo Dai[1,†]

[1] Key Laboratory of Crop Physiology Ecology and Production Management of Ministry of Agriculture, Nanjing Agricultural University, Nanjing, Jiangsu Province, 210095, P. R. China
[2] Center of Excellence for Soil Biology, College of Resources and Environment, Southwest University, Beibei, Chongqing, 400715, P. R. China
[3] College of Life Sciences, Nanjing Agricultural University, Nanjing 210095, Jiangsu Province, P. R. China

* These authors contributed equally to this work.
† Correspondence: tingbod@njau.edu.cn

Received 18 April 2018; Editorial decision 21 August 2018; Accepted 3 September 2018

Editor: Robert Sharwood, Australian National University, Australia

Abstract

Studying the response of photosynthesis to low nitrogen (N) and the underlying physiological mechanism can provide a theoretical basis for breeding N-efficient cultivars and optimizing N management. We conducted hydroponic experiments using two wheat (*Triticum aestivum*) cultivars, Zaoyangmai (low N sensitive) and Yangmai158 (low N tolerant), with either 0.25 mM N as a low N (LN) treatment or 5 mM N as a control. Under LN, a decrease in net photosynthetic rate (P_n) was attributed to reduction in the maximum Rubisco carboxylation rate, which then accelerated a reduction in the maximum ribulose-1,5-bisphosphate regeneration rate, and the reduction in P_n was 5–35% less in Yangmai158 than in Zaoyangmai. Yangmai158 maintained a 10–25% higher Rubisco concentration, especially in the upper leaves, and up-regulated Rubisco activase activity compared with Zaoyangmai to increase the Rubisco activation to sustain Rubisco carboxylation under LN conditions. In addition, Yangmai158 increased electron flux to the photorespiratory carbon oxidation cycle and alternative electron flux to maintain a faster electron transport rate and avoid photodamage. In conclusion, the LN-tolerant cultivar showed enhanced Rubisco activation and sustained electron transport to maintain a greater photosynthetic capacity under LN conditions.

Keywords: ATP, electron transport, low nitrogen, photosynthesis, Rubisco activation, winter wheat.

Introduction

Large amounts of nitrogen (N) fertilizers are applied to crops to achieve high yields worldwide. China is a major user of N fertilizers, accounting for 40% of the total global amount used, with N input doubling from 1990 to 2009; however, crop yield increased by only 22% during this period (Gong *et al.*, 2011). Only 30–40% of the N applied is utilized by plants, with

Abbreviations: CE, carboxylation efficiency; C_i, intercellular CO_2 concentration; F_v/F_m, maximum quantum efficiency of PSII; G_s, stomatal conductance; J_a, alternative electron flux; $J_{e(PCO)}$, electron flux to photorespiratory carbon oxidation; $J_{e(PCR)}$, electron flux to photosynthetic carbon reduction; J_{max}, light-saturated potential rate of electron transport; J_t, electron transport rate; I, stomatal restriction; P_n, net photosynthetic rate; PPFD, photosynthetic photon flux density; PSII, photosystem II; q_L, photochemical quenching; Rca, Rubisco activase; R_d, mitochondrial respiration rate in the light; Rubisco, ribulose-1,5-bisphosphate carboxylase/oxygenase; RuBP, ribulose-1,5-bisphosphate; V_{cmax}, maximum carboxylation rate limited by Rubisco; Γ^*, the CO_2 compensation point related to C_i; φ, apparent quantum yield; Φ_{PSII}, quantum efficiency of PSII

the majority being lost in multiple ways, including leaching, run-off, denitrification, and volatilization, placing a burden on the environment (Richter and Roelcke, 2000; Xing and Zhu, 2000; Wang *et al.*, 2016). To minimize the cost to farmers and to reduce environmental pollution, it is important to improve cultivation management to increase N-use efficiency. Wheat, one of the world's three major cereal crops, consumes more N fertilizers than any other crop (18% of the total amount) (Ladha *et al.*, 2016). In China, N-fertilizer input during wheat production can even amount to 300 kg ha^{-1} N in the north plain; however, the N-uptake efficiency is only 20–35% (Lu *et al.*, 2015). Moreover, a large amount (up to 70%) of N fertilizer is used as basal fertilizer (Shi *et al.*, 2012), but winter wheat seedlings with weak root systems and slow growth rates have a poor ability to absorb N at the seedling stage, leading to great N losses. Thus, reducing the application of basal N fertilizers could be an efficient way to increase N-use efficiency.

As N is an important component of the photosynthetic apparatus, reducing N supply may restrict photosynthetic rate (P_n), leading to reduced supply of energy and biomass, thus resulting in inhibition of tiller development and plant growth (Sage and Pearcy, 1987). However, some cultivars show higher tolerance to low N, which has a complex genetic basis (Lian *et al.*, 2005; Laperche *et al.*, 2007). Studying the different responses of cultivars with different tolerance levels would help in understanding physiological mechanisms underlying low N tolerance. Previous studies have concluded that up-regulating nitrate transporters (Jiang *et al.*, 2017), overexpressing N-assimilation-related genes (Fuentes *et al.*, 2001) and up-regulating C-metabolism-related genes (Yanagisawa *et al.*, 2004) could improve tolerance to low N. However, few reports about photosynthetic processes under low N supply are available.

Photosynthesis is a process of light-dependent and light-independent reactions. During the light-dependent reactions, light energy is absorbed by the light-harvesting complex and transported to the reaction center, where charge separation occurs. The resulting electrons are transported through the electron transport chain leading to reduction of $NADP^+$ to NADPH and photophosphorylation to produce ATP. The generated NADPH and ATP are used in the light-independent Calvin cycle in the chloroplast stroma to assimilate CO_2 into carbon compounds; ribulose-1,5-bisphosphate (RuBP) carboxylase/oxygenase (Rubisco; EC 4.1.1.39) is a key enzyme in this process. CO_2 has to overcome stomatal and mesophyll resistance to reach the carboxylation site, where it is assimilated by Rubisco (Warren, 2004). Within this highly interactive and regulated system, affecting one link causes changes to other links. Under atmospheric CO_2 conditions, the carboxylation ability of Rubisco is the key factor restricting photosynthesis (Li *et al.*, 2009; Carmo-Silva *et al.*, 2015). Under conditions of N deficiency, low Rubisco content caused by decreased N assimilation may account for reduced photosynthetic rate.

As Rubisco has a relatively low efficiency, large amounts of the enzyme are required to sustain photosynthesis, which consumes large amounts of N (Sage and Pearcy, 1987; Cheng and Fuchigami, 2000). Therefore, improving the catalytic efficiency of Rubisco may represent a viable approach to maintaining a higher photosynthetic rate under conditions of N deficiency. Carbamylation of an active site of Rubisco is a prerequisite for its activity; however, sugar phosphate can easily bind to the active site, preventing carbamylation, which may account for its inefficiency. Rubisco activase (Rca) can release tightly bound sugar phosphates from the active site to reactivate Rubisco (Carmo-Silva *et al.*, 2015). The Rca activity is mainly regulated by the ATP/ADP ratio in chloroplasts (Bracher *et al.*, 2017). Electron transport is the main process affecting ATP and ADP content in the light (Santarius and Heber, 1965), so electron transport capacity is an important factor affecting Rubisco activity.

Under low N conditions, the demand for light-dependent reaction-generated NADPH and ATP in the Calvin cycle is reduced due to a decreased carboxylation rate, which can result in overexcitation of the photosynthetic electron transport chain. As a result, PSII reaction centres will be closed and photochemical efficiency (Φ_{PSII}) and electron transport rate (J_t) decreased (Antal *et al.*, 2010). Moreover, photodamage may happen (Niyogi, 1999). Alternative electron flux driven by photorespiration and the Mehler pathway (water–water cycle) can play an important role in consuming overexcitation energy, which is considered an important photoprotection process (Demmig-Adams and Adams, 1992). Therefore, this process helps to sustain electron transport under low N conditions.

Our hypothesis is that under low N conditions, tolerant cultivars maintain faster photosynthetic rates than sensitive cultivars because of improved Rubisco carboxylation ability and sustained electron transport capacity. Increased Rubisco activation state caused by increased Rca activity may contribute to improving Rubisco carboxylation ability, while consuming excess electron in alternative electron flux may play an important role in sustaining electron transport capacity. In this study, wheat seedlings of two cultivars, Zaoyangmai [sensitive to low nitrogen (LN)] and Yangmai158 (tolerant of LN), were grown under N-sufficient (5 mM) and LN (0.25 mM) conditions. The variation in Rubisco content, Rubisco activation and electron flux were compared between the two cultivars to assess the differences in Rubisco carboxylation and electron transport capacity.

Materials and methods

Plant materials and experimental design

Two winter wheat (*Triticum aestivum* L.) cultivars, Zaoyangmai (LN sensitive) and Yangmai158 (LN tolerant) were planted for hydroponic experiments. Uniformly sized seeds of both cultivars were selected, surface sterilized with 20% (v/v) H_2O_2 for 10 min, rinsed with distilled water, and then germinated in culture dishes covered with wet sterilized gauze in the dark. When seed coleoptile length reached 1 cm, they were transferred to silica sand (soaked with 1% HCl for 2 d and flushed with copious amounts of water) and watered twice a day with distilled water. When seedlings grew to the two-leaf stage, uniform seedlings were selected and transplanted to opaque plastic containers filled with modified Hoagland nutrient solution (Li *et al.*, 2013; Jiang *et al.*, 2017) under greenhouse conditions with a photoperiod of 16 h and 18 °C day/8.5 °C night temperatures. The containers were 45 cm in length, 32 cm in width, and 15 cm in height. Each container contained 60 seedlings. The seedlings were first grown in N-sufficient solution until the four-leaf stage, and then divided into two groups. One group of seedlings was grown under N-sufficient conditions (5 mM N) as a control (CK), and the other group under LN conditions (0.25 mM N). The composition of the N-sufficient solution was as follows: 0.5 mM $Ca(NO_3)_2$, 2 mM KNO_3, 1 mM $(NH_4)_2SO_4$, 0.5 mM $CaCl_2$, 0.5 mM $CaSO_4$, 1 mM KH_2PO_4, 1 mM $MgSO_4$, 0.5 mM NaCl, 10 μM Fe-EDTA, 2.35 μM H_3BO_3, 0.55 μM

$MnSO_4{\cdot}H_2O$, 0.0385 μM $ZnSO_4{\cdot}7H_2O$, 0.0165 μM $CuSO_4{\cdot}5H_2O$, and 0.0065 μM H_2MoO_4. The composition of the low N solution was as follows: 0.075 mM $Ca(NO_3)_2$, 0.05 mM $(NH_4)_2SO_4$, 0.25 mM K_2SO_4, 0.5 mM $CaCl_2$, 0.5 mM $CaSO_4$, 1 mM KH_2PO_4, 1 mM $MgSO_4$, 0.5 mM NaCl, 10 μM Fe-EDTA, 2.35 μM H_3BO_3, 0.55 μM $MnSO_4{\cdot}H_2O$, 0.0385 μM $ZnSO_4{\cdot}7H_2O$, 0.0165 μM $CuSO_4{\cdot}5H_2O$, and 0.0065 μM H_2MoO_4. The nutrient solutions were replaced every 3 d to keep the nutrient concentrations constant, aerated continuously, and adjusted with H_2SO_4 or NaOH to maintain the pH between 5.5 and 6.0. The experiment was arranged in a completely randomized block design, with three replications for each treatment. The placement of different treatments was randomized to control for edge effects in the greenhouse.

Plant sampling

The fifth leaves were sampled at 10 d after treatment (DAT) (five-leaf stage), when P_n in LN plants decreased below the control level (Gao *et al.*, 2018), and the fifth and sixth leaves were sampled separately at 20 DAT (six-leaf stage). For each treatment, three containers were harvested as three replicates. Fresh sample was first placed in liquid N_2 for 12 h and then stored at –80 °C for chemical analysis. Plant material was dried for 20 min at 105 °C and then at 75 °C until constant weight. To determine areas of fifth and sixth leaves, they were traced on paper, and then the paper was cut and weighed, and the weight was converted to area. Total leaf area was measured using a Li-3000 area meter (Li-Cor Inc., Lincoln, NE, USA).

Gas-exchange measurements

P_n, intercellular CO_2 concentration (C_i), and stomatal conductance (G_s) were measured from 09.00 to 11.00 h using a gas exchange system (Li-Cor 6400, Li-Cor Inc.) on fifth leaves at 10 DAT and on fifth and sixth leaves at 20 DAT. Leaf temperature during measurements was maintained at 25.0 ± 0.5 °C, with steady photosynthetic photon flux density (PPFD) of 1500 μmol photons m^{-2} s^{-1}. The reference CO_2 in the cuvette was 400 ± 2.5 μmol mol^{-1}, the vapor pressure deficit (VPD) was 1.1 ± 0.05 kPa, and the relative humidity was 55–65%. Data were recorded after acclimating in the cuvette for at least 10 min. For each treatment, gas exchange measurements were determined on six plants.

Simultaneous measurements of A–C_i curves and chlorophyll fluorescence were conducted with a Li-Cor 6400 infrared gas analyser. Leaf temperature, PPFD, VPD, and relative humidity were maintained as mentioned above. Prior to measurements, leaves were placed in the cuvette at a reference CO_2 concentration of 400 μmol mol^{-1} for at least 10 min. The reference CO_2 concentration was controlled across a series of 400, 200, 150, 100, 50, 400, 600, 800, 1000, 1200, and 1500 μmol mol^{-1}, and data were recorded after CO_2 reached a steady state (2–3 min). Carboxylation efficiency (CE) was calculated as the initial slope of A–C_i curves when C_i was <200 μmol mol^{-1} (Li *et al.*, 2009).

The maximum carboxylation rate limited by Rubisco (V_{cmax}), RuBP regeneration (J_{cmax}), and stomatal limitation (l) were calculated according to a modified equation of Long and Bernacchi (2003).

Photosynthetic rate (A) is mathematically expressed as:

$$A = v_c - 0.5v_o - R_d = v_c \times \left(1 - \frac{\Gamma\star}{C_i}\right) - R_d \quad (1)$$

where v_c is the Rubisco carboxylation rate, v_o is the Rubisco oxygenation rate, R_d is the mitochondrial respiration rate in the light, and $\Gamma\star$ is the CO_2 compensation point related to the intercellular CO_2 concentration(C_i), which was measured according to the method of Li *et al.* (2009). The actual Rubisco carboxylation rate is determined by the minimum of three potential rates, the potential Rubisco carboxylation rate (w_c), the potential RuBP regeneration rate (w_j), and the potential triose phosphate utilization (TPU) rate (w_p):

$$v_c = \min\left(w_c, w_j, w_p\right) \quad (2)$$

and

$$w_c = \frac{V_{cmax} \times C_i}{C_i + K_c \times (1 + \frac{O}{K_o})} \quad (3)$$

$$w_j = \frac{J_{max} \times C_i}{4.5C_i + 10.5\Gamma\star} \quad (4)$$

$$w_p = \frac{3V_{TPU}}{1 - \frac{\Gamma\star}{C_i}} \quad (5)$$

where O is the O_2 concentration (210 mmol mol^{-1}) and V_{TPU} is the maximum rate of triose phosphate utilization.

$$K_c = \exp(38.05 - 79.43 / (R \times (T + 273.15)) \quad (6)$$

$$K_o = \exp(20.30 - 36.38 / (R \times (T + 273.15)) \quad (7)$$

where K_c and K_o are the Michaelis constants of carboxylation and oxygenation, respectively. The A–C_i curve has three phases, which can be identified by fitting J_t to C_i.

In the first phase, Rubisco is limiting and J_t increases with the increase in C_i. At this phase, Eq. (3) can be fitted to Eqs (1) and (2), and then we get:

$$A = \frac{V_{cmax} \times C_i}{C_i + K_c \times (1 + \frac{O}{K_o})} \times \left(1 - \frac{\Gamma\star}{C_i}\right) - R_d \quad (8)$$

Setting f as a variable changing with C_i:

$$f = \frac{C_i}{C_i + K_c \times (1 + \frac{O}{K_o})} \times \left(1 - \frac{\Gamma\star}{C_i}\right) \quad (9)$$

Fitting Eq. (9) to Eq. (8), Eq. (8) can be rewritten as

$$A = V_{cmax} \times f - R_d \quad (10)$$

A can be plotted as a linear function of f, where V_{cmax} was calculated as the slope and R_d was calculated as the intercept.

In the second phase, RuBP regeneration is limiting and J_t is constant with increase in C_i. Similarly, Eq. (4) can be fitted to Eqs (1) and (2):

$$A = \frac{J_{max} \times C_i}{4.5C_i + 10.5\Gamma\star} \times \left(1 - \frac{\Gamma\star}{C_i}\right) - R_d \quad (11)$$

Setting g as a variable changing with C_i:

$$g = \frac{C_i}{4.5C_i + 10.5\Gamma\star} \times \left(1 - \frac{\Gamma\star}{C_i}\right) \quad (12)$$

By fitting Eq. (12), Eq. (11) can be written as:

$$A = J_{max} \times g - R_d \quad (13)$$

Then, J_{max} was calculated as the slope.

In the third phase, TPU is limiting and J_t decreases with the increase in C_i. Frequently, TPU will not be a limitation at any C_i and so only two phases can be seen.

l was calculated from Eq. (14):

$$l = \frac{A'' - A'}{A''} \quad (14)$$

where A' is P_n at the ambient atmospheric CO_2 concentration (400 μmol mol^{-1}) and A'' is P_n when C_i is equal to ambient atmospheric CO_2 concentration (C_i=400 μmol mol^{-1}).

The light-response curves of light-adjusted leaves were measured with a Li-Cor 6400. Leaf temperature,VPD and relative humidity were maintained as mentioned above, and the reference CO_2 in the cuvette was 400 ± 2.5 μmol mol^{-1}. Prior to measurements, leaves were placed in the cuvette at a PPFD of 1500 μmol photons m^{-2} s^{-1} for at least 10 min. PPFD in the leaf cuvette was controlled across the series of 0, 50, 100, 150, and 200 μmol photons m^{-2} s^{-1} and data were recorded after reaching a steady state (2–3 min). Apparent quantum yield (φ) was calculated as the initial slope of light-response curves when PPFD was <200 μmol photons m^{-2} s^{-1} (Li *et al.*, 2009).

Chlorophyll fluorescence measurements

Chlorophyll fluorescence was measured using a Fluor-Imager (CF Imager, Technologia Ltd, Colchester, UK). The steady state fluorescence (F_s) was determined under actinic light. A saturating light pulse (~8000 μmol photons m^{-2} s^{-1}) was applied for 0.7 s to obtain the maximum fluorescence (F_m'). After removal of the actinic light and application of 3 s of far-red light, the minimal fluorescence of light-adapted state (F_o') was obtained. The minimum and maximum chlorophyll fluorescence (F_o and F_m) were determined after full dark adjustment for at least 30 min. The quantum efficiency of PSII (Φ_{PSII}) and maximum quantum efficiency of photosystem II (F_v/F_m) were calculated from Eqs (15) and (16), respectively, according to Genty *et al.* (1989):

$$\Phi_{PSII} = \frac{F_m' - F_s}{F_m'} \quad (15)$$

$$F_v / F_m = \frac{F_m - F_o}{F_m} \quad (16)$$

Photochemical quenching (q_L, in the lake model) was calculated from Eq. (17) according to Kramer *et al.* (2004):

$$q_L = \frac{F_o'}{F_s} \times \frac{F_m' - F_s}{F_m' - F_o'} \quad (17)$$

Electron transport rate (J_t) was calculated from Eq. (18) according to Li *et al.* (2009):

$$J_t = \frac{F_m' - F_s}{F_m'} \times \text{PPFD} \times 0.85 \times 0.5 \quad (18)$$

Calculation of the electron flux to the photosynthetic carbon reduction cycle, electron flux to the photorespiratory carbon oxidation cycle, and alternative electron flux

The electron fluxes in the photosynthetic carbon reduction cycle ($J_{e(PCR)}$), photorespiratory carbon oxidation cycle ($J_{e(PCO)}$), and alternative electron flux (J_a) were calculated form Eqs (19), (20), and (21) according to Zhou *et al.* (2004):

$$J_{e(PCR)} = 4 \times v_c = 4 \times \frac{A + R_d}{1 - \frac{\Gamma^\star}{C_i}} \quad (19)$$

$$J_{e(PCO)} = 4 \times v_o = 2 \times \frac{\Gamma^\star}{C_i} \quad (20)$$

$$J_a = J_t - J_{e(PCR)} - J_{e(PCO)} \quad (21)$$

Determination of Rubisco concentration

The Rubisco concentration was determined according to the method of Makino *et al.* (1986), with minor modifications, using SDS-PAGE. Frozen leaves (10 cm^2) were homogenized in 5 ml of 50 mM Tris–HCl buffer (pH 7.6) containing 5 mM 2-mercaptoethanol, 12.5% (v/v) glycerol, 1 mM $MgCl_2$, and 1 mM EDTA. The mixture was centrifuged at 10 000 *g* (4 °C) for 15 min. Next, 2 ml of crude enzyme was mixed with 0.5 ml of 5×loading buffer (pH 6.8) containing 1 mM Tris, 2% (w/v) SDS, 5% (v/v) 2-mercaptoethanol, 25% (v/v) glycerol, and 0.1% (w/v) bromophenol blue, and the mixture was boiled for 5 min. Then, 10 μl of this preparation, which was heated to 65 °C for 10 min and centrifuged at 1800 *g* for 15 min in advance, was used for electrophoresis at 100 V for about 7 h. After electrophoresis, gels were stained with 0.25% (w/v) Coomassie Brilliant Blue R-250 for visualization and destained with destaining solution (25% ethanol–8% glacial acetic acid) until the background became colorless. Large subunits (55 kDa) and small subunits (15 kDa) were transferred into a 10 ml cuvette with 2 ml of formamide and washed in a 50 °C water bath at room temperature overnight; the absorbance was measured at 595 nm to determine protein content in the bands.

Determination of Rubisco activase concentration

The Rca concentration was measured by ELISA (Choi and Roh, 2003), using a Rubisco activase enzyme-linked immunosorbent assay (ELISA) Kit (Jianglai Biology, Shanghai, China). Fifty microliters of crude extract and 100 μl of rabbit anti-Rubisco activase antiserum were added to wells of a 96-well microtiter plate, which were pre-coated with the Rca antigen, and incubated for 30 min at 37 °C. Then the plate was washed and 100 μl of peroxidase-conjugated goat anti-rabbit IgG was added and incubated for 30 min at 37 °C. After the plate was washed again, 100 μl of peroxidase substrate was added. After incubation at room temperature in the dark for 20 min, the reaction was terminated by adding 0.1 ml of 1 M HCl. Absorbance at 490 nm was determined by an ELISA microplate reader (Bio-Rad model 3550-UV).

Determination of Rubisco and Rca activity

Rubisco activity was measured spectrophotometrically by coupling RuBP carboxylation to NADH oxidation (Sharwood *et al.*, 2016). Frozen leaves (1 cm^2) were homogenized in 1 ml of ice cold, N_2-sparged 50 mM EPPS–NaOH buffer (pH 8.0) containing 0.5 mM EDTA, 10 mM $MgCl_2$, 5 mM dithiothreitol, and 1% (w/v) polyvinylpolypyrrolidone. The mixture was rapidly centrifuged at 15 000 *g* (4 °C) for 1 min. Twenty microliters of crude extract was assayed rapidly for initial Rubisco activity in 1 ml cuvettes containing 0.46 ml of assay buffer (100 mM EPPS–NaOH, pH 8.0, 10 mM $MgCl_2$, 1 mM EDTA, 0.2 mM NADH, 20 mM $NaHCO_3$, 5 mM dithiothreitol, 5 mM ATP, 10 U ml^{-1} creatine phosphokinase, 10 U ml^{-1} 3-phosphoglyceric phosphokinase, 10 U ml^{-1} glyceraldehyde-3-phosphate dehydrogenase and 5 mM phosphocreatine) and 20 μl of 10 mM RuBP. Change in absorbance at 340 nm was monitored for 60 s at 25 °C. To measure total Rubisco activities, 20 μl of crude enzyme was first activated for 10 min at 25 °C in RuBP-free assay buffer before starting Rubisco activity measurements by adding 20 μl of 10 mM RuBP. The Rubisco activation state was calculated as the ratio of initial activity to total activity.

Rca activity was measured according to the method of Carmo-Silva and Salvucci (2011) with minor modifications. Briefly, Rubisco in the extracts was supplemented with 5% polyethylene glycol 3350 and 4 mM RuBP and incubated for 5 min at 4 °C to promote the formation of inactive Rubisco–RuBP (ER) complex. The extract was then added to equal volume of reactivation solution (containing 90 mM Tris–HCl, pH 7.5, 40 mM $MgCl_2$ and 20 mM $NaHCO_3$ with or without 10 mM ATP and an ATP-regenerating system consisting of 10 mM phosphocreatine and 200 U ml^{-1} phosphocreatine kinase) and incubated for 5 min at 25 °C. The Rubisco activity was measured subsequently and compared with total Rubisco activity to calculate the fraction of Rubisco active sites that were restored to catalytic competence. The Rca activity was determined as the increase of the fraction of active sites per minute after subtracting the spontaneous rate of activation determined by measuring Rubisco activity in the reactions without ATP and ATP regeneration system.

Determination of ATP and ADP concentration

The ATP and ADP concentrations were measured using an ATP Assay Kit and ADP Assay Kit (Detect Technical Institute, Shanghai, China) according to the manufacturer's instructions (Wang *et al.*, 2013). The working solution was prepared according to the kit protocol. Then, 100 µl of working solution and 100 µl of crude extract were added to each well of a 96-well microtiter plate. The luciferase signal was detected by a multifunctional microplate reader (SpectraMax M2) for 30 s. ADP concentration was measured after ADP was converted to ATP.

Statistical analysis

A two-way analysis of variance (ANOVA) with Dunnett's multiple comparison test was conducted using SPSS software version 19 (IBM Corp., Armonk, NY, USA) to determine the significance of the effects of different cultivars and N levels. Graphs were plotted using SigmaPlot 10.0 software (Systat Software, Inc., San Jose, CA, USA).

Results

Dry weight and leaf area

The LN treatment resulted in a significant reduction in shoot and plant (shoot+root) biomass of both cultivars at 20 DAT, and the shoot biomass was reduced by 45% for Zaoyangmai, but only 23% for Yangmai158 (Table 1). On the contrary, growth in LN conditions induced a significant increase in root weight of Yangmai158, whereas the increase was not prominent in Zaoyangmai. Moreover, LN also reduced leaf area, and the reduction was greater in Zaoyangmai than in Yangmai158. In Zaoyangmai, LN reduced the fifth leaf, sixth leaf, and total leaf area by an average of 17%, 49%, and 48%, respectively, compared with CK. However, the average reduction of the fifth leaf, sixth leaf, and total leaf area was only 5%, 18%, and 38%, respectively, in Yangmai158.

Photosynthesis and its related attributes

The LN treatment reduced P_n in both cultivars compared with CK (Fig. 1), but the reduction in Yangmai158 was less than that in Zaoyangmai. Moreover, the extent of reduction of P_n in the sixth leaf was less than that in the fifth leaf in Yangmai158 at 20 DAT, and this phenomenon was not prominent in Zaoyangmai. At 20 DAT under LN conditions, P_n of the fifth and sixth leaves was 55% and 51% lower, respectively, in Zaoyangmai than in CK, whereas the reduction of P_n in Yangmai158 was much less in the sixth leaf (17%) than in the fifth leaf (30%).

Compared with CK, LN treatment significantly decreased G_s (Fig. 1) in both cultivars, but increased C_i (Fig. 1) and l (Table 2) in both cultivars, indicating that although LN led to a decrease in G_s, the C_i was sufficient and would not restrict photosynthesis. At 10 DAT, wheat plants had significantly lower CE and V_{cmax} values when grown under LN, and these effects were especially notable for Zaoyangmai (Table 2). However, LN did not reduce φ or J_{max} at this time (Table 2). At 20 DAT, LN reduced CE, φ, V_{cmax}, and J_{max}, and these reductions were greater in Zaoyangmai than in Yangmai158. At 20 DAT, LN reduced CE, φ, V_{cmax}, and J_{max} in the fifth leaf of Zaoyangmai by 54%, 51%, 34%, and 33%, but only 40%, 30%, 21%, and 13% in the fifth leaf of Yangmai158 compared with that of CK. Moreover, no significant reductions in φ or J_{max} were observed in the sixth leaf of Yangmai158.

Rubisco carboxylation section

The Rubisco concentration decreased markedly in plants grown under LN (Fig. 2), but the decrease was much greater in Zaoyangmai (41% at 10 DAT) than in Yangmai158 (30% at 10 DAT). Moreover, at 20 DAT, the decrease in Rubisco concentration was less in the sixth leaf than in the fifth leaf, particularly in Yangmai158. Compared with CK, the Rubisco concentration of Yangmai158 decreased by 37% in the fifth leaf and only 24% in the sixth leaf under LN, while that of Zaoyangmai decreased by 50% in the fifth leaf and 48% in the sixth leaf.

The LN treatment resulted in decreases in the initial Rubisco activity and total Rubisco activity in both cultivars (Fig. 3). At 20 DAT, LN reduced initial Rubisco activity in the fifth and sixth leaves in Zaoyangmai by an average of 49% and 38%, respectively, compared with CK. The average reductions of the fifth and sixth leaves were only 29% and 11%, respectively, in Yangmai158. However, growth under LN induced significant increases in the Rubisco activation state in both cultivars (Fig. 3), but the extent of the increase was much less in Zaoyangmai (7% in the fifth leaf and 13% in the sixth leaf at 20 DAT) than in Yangmai158 (15% in the fifth leaf and 22% in the sixth leaf at 20 DAT).

No significant effect of LN on Rca concentration was observed in either cultivar (Fig. 4). In contrast, Rca activity increased significantly in both cultivars grown under LN (Fig. 4), but the extent of the increase was less in Zaoyangmai (12% in the fifth leaf and 24% in the sixth leaf at 20 DAT) than in Yangmai158 (36% in the fifth leaf and 41% in the sixth leaf at 20 DAT).

Electron transport section

The LN reduced ATP and ADP concentrations in both cultivars (Fig. 5), but the reductions were less in Yangmai158 than in Zaoyangmai. In contrast, the ATP/ADP ratios increased

Table 1. *Effects of nitrogen deficiency on dry weight and leaf area of wheat seedlings at 20 d after treatment*

Cultivar	Treatment	Shoot dry weight (mg plant^{-1})	Root dry weight (mg plant^{-1})	Plant dry weight (mg plant^{-1})	Fifth leaf area (cm^2 plant^{-1})	Sixth leaf area (cm^2 plant^{-1})	Plant leaf area (cm^2 plant^{-1})
Zaoyangmai	CK	1062 ± 56a	280 ± 6b	1342 ± 61a	7.3 ± 0.1c	12.4 ± 0.6c	324 ± 7a
	LN	589 ± 10c	301 ± 11b	890 ± 10c	6.1 ± 0.1d	6.6 ± 0.1d	167 ± 6c
Yangmai158	CK	1135 ± 46a	284 ± 10b	1418 ± 54a	12.6 ± 0.1a	22.9 ± 0.2a	343 ± 9a
	LN	866 ± 33b	335 ± 7a	1201 ± 38b	11.1 ± 0.1b	19.8 ± 0.3b	213 ± 5b

Data are expressed as means ±SE, n=6. Lowercase letters following the data within the same column refer to significant differences (P<0.05), which were determined by Dunnett's multiple comparison test.

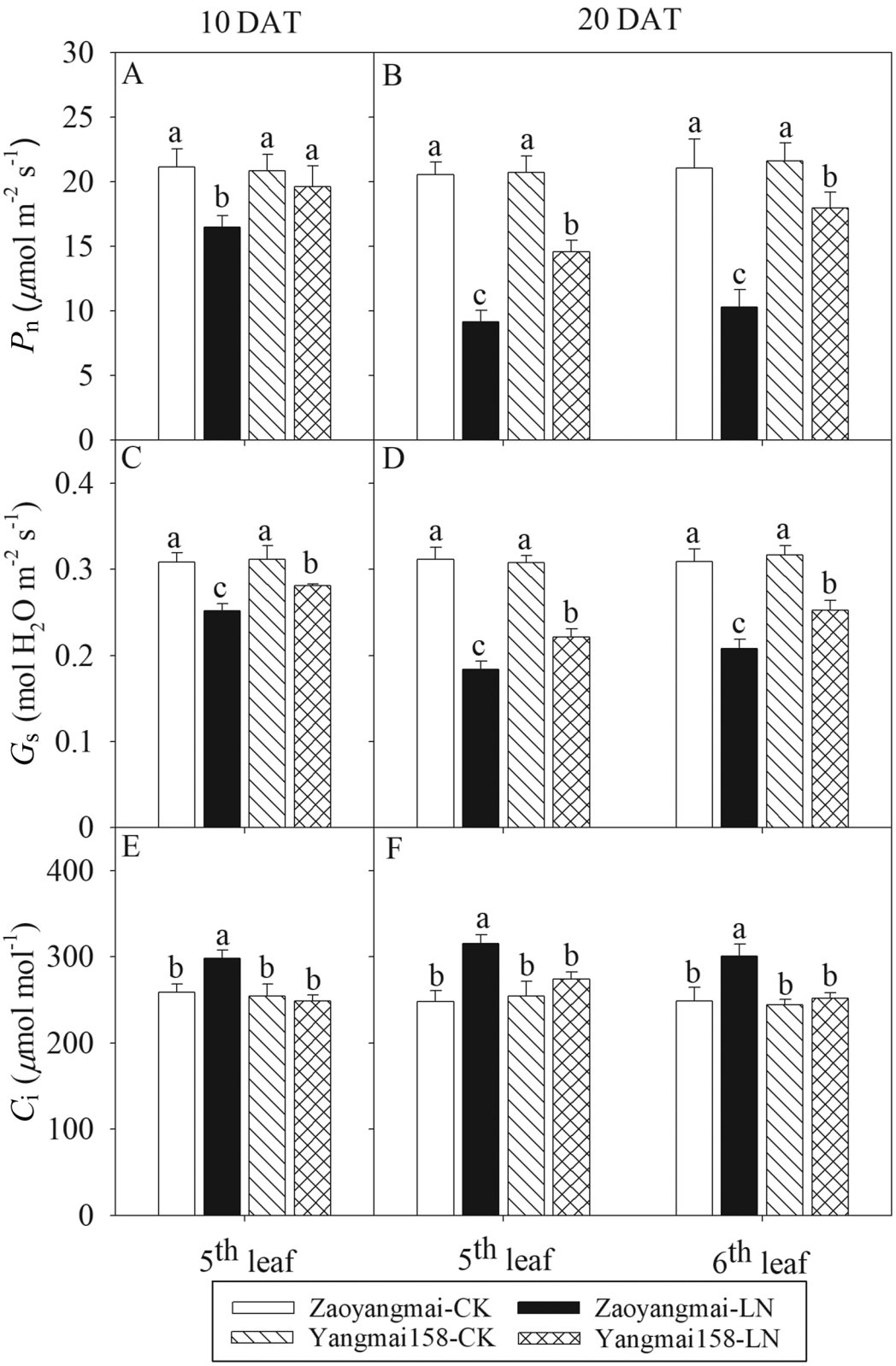

Fig. 1. Effects of nitrogen deficiency on P_n, G_s, and C_i in newly expanded leaves of wheat seedlings at 10 and 20 d after treatment (DAT). Data are expressed as means over six replicates. Lowercase letters indicate significant difference at the 0.05 level, determined by Dunnett's multiple comparison test. Error bars indicate SE.

significantly in plants grown under LN (Fig. 5), and the increase was much greater in Yangmai158 (16% in the fifth leaf and 25% in the sixth leaf at 20 DAT) than in Zaoyangmai (10% in the fifth leaf and 8% in the sixth leaf at 20 DAT).

Corresponding to ATP concentration, J_t decreased in both cultivars under LN compared with CK (Table 3), and this reduction was more significant in Zaoyangmai (45% in the fifth leaf and 29% in the sixth leaf at 20 DAT) than in Yangmai158

Table 2. *Effects of nitrogen deficiency on CE, φ, V_{cmax}, J_{max}, and I in newly expanded leaves of wheat seedlings at 10 and 20 d after treatment (DAT)*

		Cultivar	Treatment	CE	φ	V_{cmax} (μmol m^{-2} s^{-1})	J_{max} (μmol m^{-2} s^{-1})	I
10 DAT	Fifth leaf	Zaoyangmai	CK	0.131 ± 0.002a	0.056 ± 0.002a	47.1 ± 1.3a	196.4 ± 6.9a	0.278 ± 0.003a
			LN	0.120 ± 0.005b	0.053 ± 0.001a	40.0 ± 0.6b	195.6 ± 4.9a	0.253 ± 0.003b
		Yangmai158	CK	0.130 ± 0.003ab	0.057 ± 0.001a	46.2 ± 0.9a	193.1 ± 4.0a	0.280 ± 0.002a
			LN	0.129 ± 0.001ab	0.056 ± 0.002a	44.1 ± 0.9a	199.5 ± 1.7a	0.252 ± 0.003b
20 DAT	Fifth leaf	Zaoyangmai	CK	0.133 ± 0.003a	0.057 ± 0.001a	47.9 ± 1.0a	201.6 ± 4.0a	0.277 ± 0.003a
			LN	0.061 ± 0.005c	0.028 ± 0.002c	31.6 ± 0.2c	134.6 ± 3.7c	0.187 ± 0.006c
		Yangmai158	CK	0.131 ± 0.002a	0.054 ± 0.002a	46.4 ± 1.5a	200.5 ± 6.3a	0.285 ± 0.005a
			LN	0.078 ± 0.004b	0.038 ± 0.001b	36.5 ± 0.5b	175.2 ± 2.7b	0.216 ± 0.005b
	Sixth leaf	Zaoyangmai	CK	0.130 ± 0.002a	0.056 ± 0.001a	46.9 ± 1.3ab	206.2 ± 3.5a	0.294 ± 0.017a
			LN	0.067 ± 0.002c	0.038 ± 0.003c	35.2 ± 0.3c	162.4 ± 3.8b	0.193 ± 0.006c
		Yangmai158	CK	0.134 ± 0.002a	0.055 ± 0.001a	48.7 ± 0.8a	198.3 ± 6.9a	0.281 ± 0.003a
			LN	0.111 ± 0.002b	0.050 ± 0.002a	44.3 ± 0.7b	189.3 ± 4.7a	0.238 ± 0.003b

Data are expressed as means ±SE, *n*=6. Lowercase letters following the data within the same column refer to significant differences ($P<0.05$), which were determined by Dunnett's multiple comparison test.

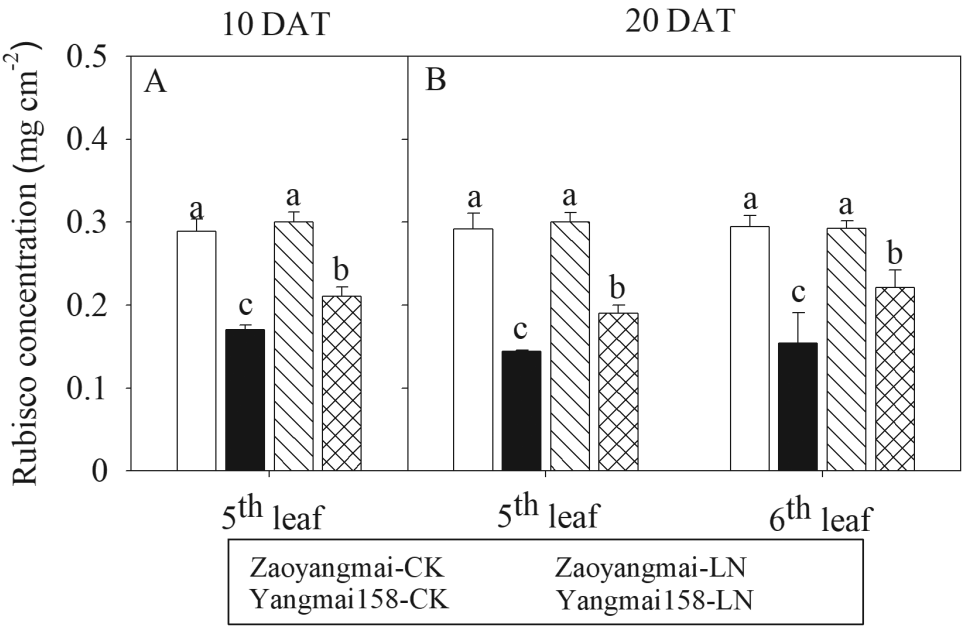

Fig. 2. Effects of nitrogen deficiency on Rubisco concentration in newly expanded leaves of wheat seedlings at 10 and 20 d after treatment (DAT). Data are expressed as means over six replicates. Lowercase letters indicate significant difference at the 0.05 level, determined by Dunnett's multiple comparison test. Error bars indicate SE.

(14% in the fifth leaf and 3% in the sixth leaf at 20 DAT). The LN resulted in significant reductions in Φ_{PSII} and q_L in both cultivars (Table 3), and these reductions were more significant in Zaoyangmai than in Yangmai158. At 20 DAT, the reduction of q_L in the fifth and the sixth leaves of Zaoyangmai was 37% and 19%, respectively, under LN compared to CK, while that of Yangmai158 was only 25% and 7%, respectively. Under LN conditions, F_v/F_m showed no significant difference from the control at 10 DAT. However, at 20 DAT, F_v/F_m decreased under LN in the fifth leaves of Zaoyangmai (Table 3), while that in Yangmai158 remained at the CK level.

Under LN, $J_{e(PCR)}$ and $J_{e(PCO)}$ decreased in both cultivars (Table 3), but $J_{e(PCR)}$ and $J_{e(PCO)}$ in Yangmai158 were higher than in Zaoyangmai. Moreover, the $J_{e(PCR)}/J_t$ ratio decreased under LN; at 20 DAT, the $J_{e(PCR)}/J_t$ ratio in the sixth leaf of Zaoyangmai was 69% and 59% in CK and LN, respectively, while that of Yangmai158 was 68% and 62% in CK and LN, respectively. In contrast, LN resulted in increases in J_a in both cultivars (Table 3), and the increase was more significant in Yangmai158 (93% in the fifth leaf and 75% in the sixth leaf at 20 DAT) than in Zaoyangmai (31% in the fifth leaf and 50% in the sixth leaf at 20 DAT).

Discussion

Hydroponic experiments have advantages over field or pot experiments when conducting investigations that require precision, as complex interactions between ions and soil particles may affect nutrient bioavailability (Conn *et al.*, 2013; Nguyen *et al.*, 2016). In this study, a hydroponic experiment was conduct to study the response of wheat seedlings to LN. The ability of wheat seedlings to withstand N deficiency stress differed

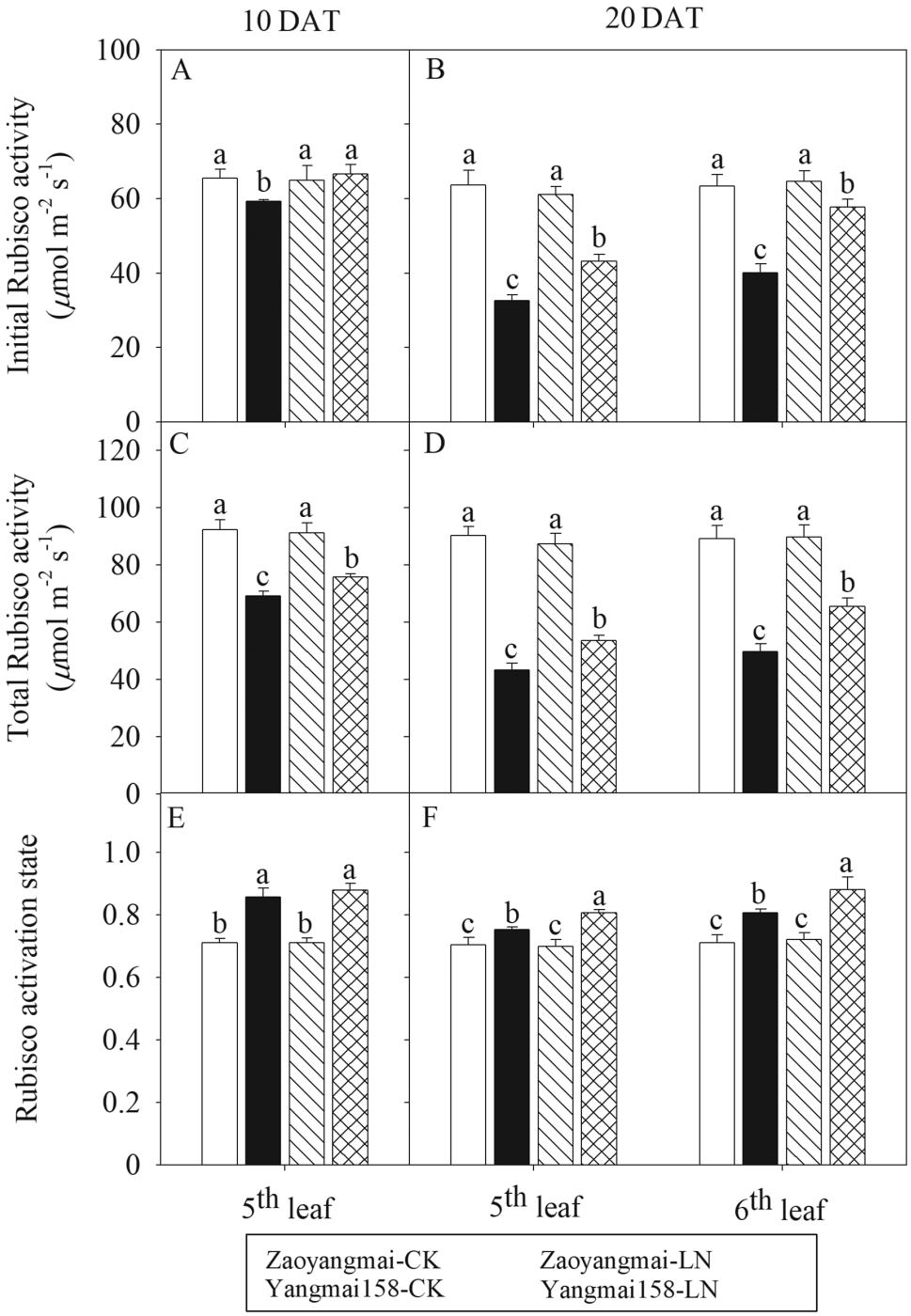

Fig. 3. Effects of nitrogen deficiency on initial Rubisco activity, total Rubisco activity and Rubisco activation state in newly expanded leaves of wheat seedlings at 10 and 20 d after treatment (DAT). Data are expressed as means over six replicates. Lowercase letters indicate significant difference at the 0.05 level, determined by Dunnett's multiple comparison test. Error bars indicate SE.

between cultivars. The most obvious response of plants to N deficiency was observed as decreased P_n (Fig. 1) leading to reduced plant dry weight and leaf area (Table 1). However, Yangmai158 showed lower reduction of P_n than Zaoyangmai from sufficient nitrogen to low nitrogen conditions, especially in the upper leaves, leading to a higher dry matter.

As photosynthesis is a highly synergistic system—affecting one link causes changes to other links—the factors responsible for the decrease in photosynthesis under LN conditions remain controversial. To identify the primary target of the LN-induced decrease in rate of photosynthesis, we examined stomatal limitation and photochemical reactions. Wheat plants exposed to LN showed lower G_s (Fig. 1) than CK plants; however, C_i (Fig. 1) increased and l (Table 2) decreased under LN. It was concluded by Li *et al.* (2015) that increased C_i when G_s declined was caused by a decrease in the rate of the photosynthetic CO_2 reduction. In this study, at 20 DAT, LN resulted in reduction of both V_{cmax} and J_{max} (Table 2), while at 10 DAT LN had little effect on J_{max} but resulted in decreased V_{cmax}. Sage (1990) concluded that non-limiting processes can be regulated

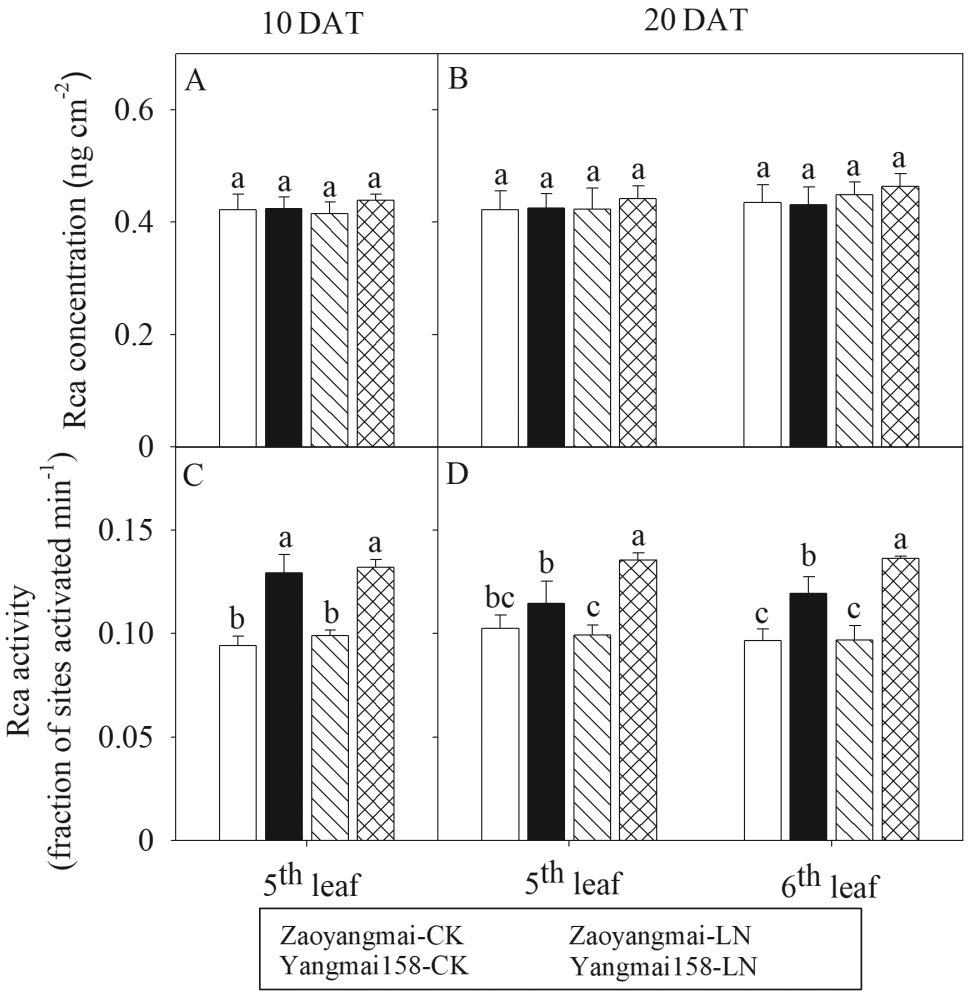

Fig. 4. Effects of nitrogen deficiency on Rca concentration and Rca activity in newly expanded leaves of wheat seedlings at 10 and 20 d after treatment (DAT). Data are expressed as means over six replicates. Lowercase letters indicate significant difference at the 0.05 level, determined by Dunnett's multiple comparison test. Error bars indicate SE.

to match the ability of limiting processes in the photosynthetic system. Therefore, after N withdrawal, the decrease in P_n was first attributed to the decrease in Rubisco carboxylation ability, which then accelerated the decrease of electron transport capacity, confirming some studies showing that reduction in chlorophyll and Rubisco content results in decreased photochemical efficiency, leading to a decreased photosynthetic rate (Ciompi *et al.*, 1996; Shangguan *et al.*, 2000; Cruz *et al.*, 2003).

The V_{cmax} reflects apparent Rubisco activity *in vivo*, which depends on both the amount of Rubisco and its activation state (Long and Bernacchi, 2003). Our results show that Rubisco concentration decreased significantly under LN (Fig. 2), which should be responsible for the decrease in V_{cmax}. Compared with the LN-sensitive cultivar, the LN-tolerant cultivar maintained a higher Rubisco concentration under LN, especially in upper leaves. Our previous study indicated that Yangmai158 had higher N absorption ability than Zaoyangmai, because of root extension and nitrate transporter up-regulation (Jiang *et al.*, 2017), which would contribute to improved N status and Rubisco synthesis.

Previous studies indicated that the Rubisco activation state increased at low N supply (Mächler *et al.*, 1988), which can be an important mechanism for acclimation to low N environments. In this study, the Rubisco activation state increased significantly under LN (Fig. 3), particularly in Yangmai158; as a result, the extent of decrease in P_n (16% in the sixth leaf of Yangmai158 at 20 DAT) was less than in Rubisco concentration (24% in the sixth leaf of Yangmai158 at 20 DAT). Therefore, exploring the gene related to optimizing Rubisco may provide a genetic basis for low nitrogen tolerance research. Rca relieves the contact inhibition of sugar phosphate inhibitors and promotes carbamylation to improve Rubisco activity, and the manipulation of Rca is considered an effective way to regulate Rubisco activity (Bracher *et al.*, 2017). In this study, LN resulted in promotion of Rca activity, but had no significant effect on the Rca concentration (Fig. 4). The Rca activity is regulated mainly by the ATP/ADP ratio (Carmo-Silva *et al.*, 2015). In comparison, the LN-induced improvement of Rca activity was accompanied by an increase in the ATP/ADP ratio (Fig. 5) consistent with the results of Mächler *et al.* (1988). This may be due to the lower consumption of ATP by the Calvin cycle and N metabolism. However, Yangmai158 possessing higher Rubisco carboxylation ability had a higher ATP/ADP ratio than Zaoyangmai under LN conditions, indicating that it had a higher capacity to synthesize ATP.

ATP synthesis plays an important role in feedback regulatory mechanisms, sensing stress-induced changes in metabolic

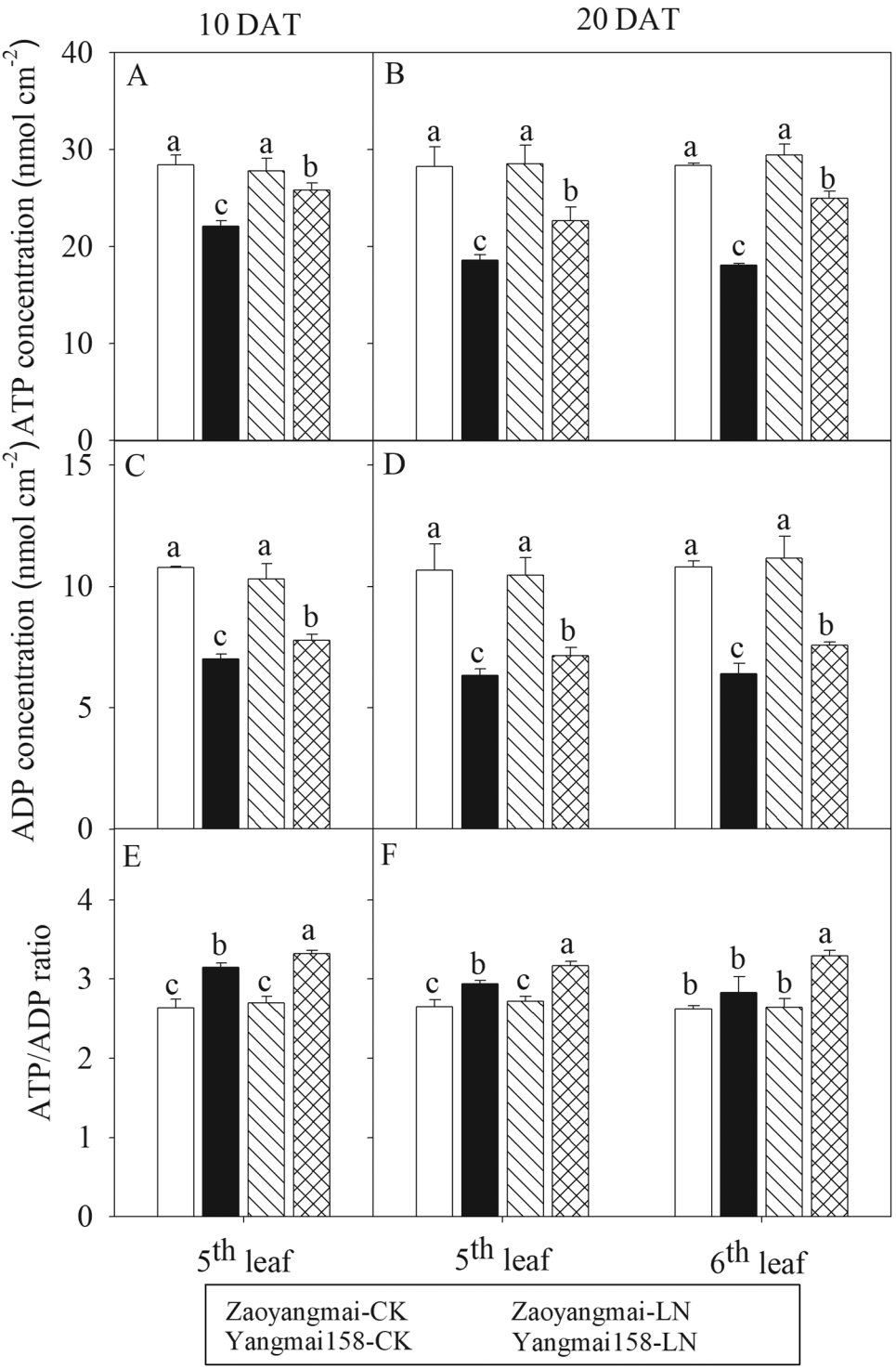

Fig. 5. Effects of nitrogen deficiency on ATP and ADP concentration and ATP/ADP ratio in newly expanded leaves of wheat seedlings at 10 and 20 d after treatment (DAT). Data are expressed as means over six replicates. Lowercase letters indicate significant difference at the 0.05 level, determined by Dunnett's multiple comparison test. Error bars indicate SE.

status, and then adjusting light capture and electron transport, and consequently regulating other metabolic pathways (Kohzuma *et al.*, 2013). The photosynthetic electron transport reaction generates a proton-motive force, driving the phosphorylation of ADP to ATP, which is the main pathway involved in synthesis of ATP in the light (Armbruster *et al.*, 2017). Under N-deficient conditions, the loss of carboxylation efficiency of Rubisco would lead to reduced capacity for consuming NADPH and regenerating $NADP^+$, resulting in a lack of electron receptors, which would in turn shut down PSII. Our results show that LN resulted in significant closure of PSII, identified by decreased q_L (Kramer *et al.*, 2004). As a result, Φ_{PSII} and J_t decreased (Table 3). When absorbed light energy exceeds the capacity for energy dissipation, the PSII reaction centers are at risk of damage (Niyogi, 1999). As shown in our results, under LN, F_v/F_m decreased in Zaoyangmai

Table 3. *Effects of nitrogen deficiency on Φ_{PSII}, q_L, F_v/F_m, J_t, $J_{e(PCR)}$, $J_{e(PCO)}$, and J_a in newly expanded leaves of wheat seedlings at 10 and 20 d after treatment (DAT)*

	Cultivar	Treatment	Φ_{PSII}	q_L	F_v/F_m	J_t (μmol e^{-1} m^{-2} s^{-1})	$J_{e(PCR)}$ (μmol e^{-1} m^{-2} s^{-1})	$J_{e(PCO)}$ (μmol e^{-1} m^{-2} s^{-1})	J_a (μmol e^{-1} m^{-2} s^{-1})
10 DAT	Fifth leaf	Zaoyangmai	CK	0.314 ± 0.003a	0.305 ± 0.011ab	0.824 ± 0.005a	160.3 ± 1.7a	107.2 ± 1.5a	40.4 ± 1.5a	12.7 ± 0.5ab
			LN	0.261 ± 0.005c	0.281 ± 0.005c	0.821 ± 0.004a	133.3 ± 2.4c	90.7 ± 2.3c	31.8 ± 0.8b	10.8 ± 2.0b
		Yangmai158	CK	0.309 ± 0.007ab	0.306 ± 0.011a	0.817 ± 0.009a	157.7 ± 3.7ab	106.4 ± 1.3a	38.8 ± 2.5a	12.5 ± 0.9ab
			LN	0.301 ± 0.002b	0.293 ± 0.008bc	0.816 ± 0.014a	153.6 ± 1.0b	101.8 ± 0.7b	38.4 ± 1.7a	13.5 ± 1.4a
20 DAT	Fifth leaf	Zaoyangmai	CK	0.309 ± 0.003a	0.303 ± 0.012a	0.818 ± 0.010a	157.4 ± 1.7a	102.7 ± 1.8a	41.4 ± 0.1a	13.2 ± 1.6c
			LN	0.169 ± 0.006c	0.191 ± 0.014c	0.746 ± 0.013b	86.2 ± 3.0c	46.2 ± 1.5c	22.6 ± 2.1c	17.4 ± 0.8b
		Yangmai158	CK	0.307 ± 0.008a	0.300 ± 0.007a	0.816 ± 0.006a	156.5 ± 4.0a	106.7 ± 0.8a	37.7 ± 1.3a	12.0 ± 2.1c
			LN	0.263 ± 0.009b	0.225 ± 0.020b	0.814 ± 0.008a	134.2 ± 4.7b	82.5 ± 2.8b	28.6 ± 2.5b	23.2 ± 0.8a
	Sixth leaf	Zaoyangmai	CK	0.302 ± 0.002ab	0.307 ± 0.009a	0.816 ± 0.012a	153.9 ± 1.0ab	105.4 ± 1.8a	37.4 ± 0.8a	11.0 ± 2.4c
			LN	0.215 ± 0.005c	0.250 ± 0.002c	0.783 ± 0.009b	109.6 ± 2.8c	65.1 ± 2.7c	27.6 ± 1.8c	16.8 ± 1.4b
		Yangmai158	CK	0.306 ± 0.005a	0.309 ± 0.012a	0.815 ± 0.011a	156.0 ± 2.3a	105.7 ± 0.3a	37.9 ± 1.2a	12.4 ± 2.8c
			LN	0.298 ± 0.001b	0.287 ± 0.005b	0.811 ± 0.011a	151.7 ± 0.6b	95.3 ± 2.1b	34.8 ± 1.9b	21.6 ± 2.4a

Data are expressed as means ±SE, *n*=6. Lowercase letters following the data within the same column refer to significant differences ($P<0.05$), which were determined by Dunnett's multiple comparison test.

compared with CK at 20 DAT (Table 3), indicating damage to PSII may occur. Compared with Zaoyangmai, Yangmai158 had a greater ability to maintain open PSII to allow electron transport to proceed more smoothly. Moreover, LN caused no damage to the reaction centers in Yangmai158.

Electron transport to oxygen through the photorespiratory or Mehler pathway (water–water cycle) plays an important role in consuming excess excitation energy, and maintaining open PSII (Demmig-Adams and Adams, 1992; Niyogi, 1999). Under LN, the $J_{e(PCR)}/J_t$ ratio decreased compared with CK, indicating increasing electron flux to oxygen. Although photorespiration is an ATP-consuming process, it is capable of maintaining the open PSII reaction centers and linear electron transport under conditions of carboxylation limitation (Makino, 2011). The Mehler pathway generates a proton-motive force for ATP synthesis, but produces neither NADPH nor O_2 (Miyake and Yokota, 2000). In this study, Yangmai158 had higher $J_{e(PCO)}$ and J_a compared with Zaoyangmai under LN conditions (Table 3), indicating proper functioning of alternative electron flux to photorespiratory and Mehler pathways, explaining why Yangmai158 had a greater ability to maintain open PSII. However, the $J_{e(PCR)}/J_t$ ratio was still higher in Yangmai158 than in Zaoyangmai under LN, indicating Yangmai158 invested more energy in photosynthetic carbon assimilation than Zaoyangmai.

In conclusion, under low N conditions, Rubisco carboxylation ability decreased leading to suppression of photosynthesis that would further lead to a reduction in electron transport capacity. However, a low N tolerant cultivar maintained Rubisco carboxylation by improving Rubisco activation and sustaining electron transport by consuming excess excitation energy through photorespiratory and Mehler pathways, which contributed to sustained photosynthesis under low N conditions. In the future, Rca may be an effective target for breeding low N tolerant cultivars, which will contribute to low N input agriculture.

Acknowledgements

We acknowledge grant from the National Natural Science Foundation of China (Grant no. 31471443, 31501262) and a Project Funded by the Priority Academic Program Development of Jiangsu Higher Education Institutions (PAPD). Moreover, the authors would like to thank professor Hans Lambers (School of Biological Sciences, University of Western Australia) for guidance in writing of the manuscript.

References

Antal T, Mattila H, Hakala-Yatkin M, Tyystjärvi T, Tyystjärvi E. 2010. Acclimation of photosynthesis to nitrogen deficiency in *Phaseolus vulgaris*. Planta **232,** 887–898.

Armbruster U, Correa Galvis V, Kunz HH, Strand DD. 2017. The regulation of the chloroplast proton motive force plays a key role for photosynthesis in fluctuating light. Current Opinion in Plant Biology **37,** 56–62.

Bracher A, Whitney SM, Hartl FU, Hayer-Hartl M. 2017. Biogenesis and metabolic maintenance of Rubisco. Annual Review of Plant Biology **68,** 29–60.

Carmo-Silva AE, Salvucci ME. 2011. The activity of Rubisco's molecular chaperone, Rubisco activase, in leaf extracts. Photosynthesis Research **108,** 143–155.

Carmo-Silva E, Scales JC, Madgwick PJ, Parry MA. 2015. Optimizing Rubisco and its regulation for greater resource use efficiency. Plant, Cell & Environment **38,** 1817–1832.

Cheng L, Fuchigami LH. 2000. Rubisco activation state decreases with increasing nitrogen content in apple leaves. Journal of Experimental Botany **51,** 1687–1694.

Choi BY, Roh KS. 2003. UV-B radiation affects chlorophyll and activation of Rubisco by Rubisco activase in *Canavalia ensiformis* L. leaves. Journal of Plant Biology **46,** 117.

Ciompi S, Gentili E, Guidi L, Soldatini GF. 1996. The effect of nitrogen deficiency on leaf gas exchange and chlorophyll fluorescence parameters in sunflower. Plant Science **118,** 177–184.

Conn SJ, Hocking B, Dayod M, *et al*. 2013. Protocol: optimising hydroponic growth systems for nutritional and physiological analysis of *Arabidopsis thaliana* and other plants. Plant Methods **9,** 4.

Cruz J, Mosquim P, Pelacani C, Araújo W, DaMatta F. 2003. Photosynthesis impairment in cassava leaves in response to nitrogen deficiency. Plant and Soil **257,** 417–423.

Demmig-Adams B, Adams W III. 1992. Photoprotection and other responses of plants to high light stress. Annual Review of Plant Biology **43,** 599–626.

Fuentes SI, Allen DJ, Ortiz-Lopez A, Hernández G. 2001. Over-expression of cytosolic glutamine synthetase increases photosynthesis and growth at low nitrogen concentrations. Journal of Experimental Botany **52,** 1071–1081.

Gao J, Wang F, Hu H, *et al*. 2018. Improved leaf nitrogen reutilisation and Rubisco activation under short-term nitrogen-deficient conditions promotes photosynthesis in winter wheat (*Triticum aestivum* L.) at the seedling stage. Functional Plant Biology **45,** 840–853.

Genty B, Briantais JM, Baker NR. 1989. The relationship between the quantum yield of photosynthetic electron transport and quenching of chlorophyll fluorescence. Biochimica et Biophysica Acta **990,** 87–92.

Gong P, Liang L, Zhang Q. 2011. China must reduce fertilizer use too. Nature **473,** 284–285.

Jiang S, Sun J, Tian Z, Hu H, Michel EJS, Gao J, Jiang D, Cao W, Dai T. 2017. Root extension and nitrate transporter up-regulation induced by nitrogen deficiency improves nitrogen status and plant growth at the seedling stage of winter wheat (*Triticum aestivum* L.). Environmental and Experimental Botany **141,** 28–40.

Kohzuma K, Dal Bosco C, Meurer J, Kramer DM. 2013. Light- and metabolism-related regulation of the chloroplast ATP synthase has distinct mechanisms and functions. The Journal of Biological Chemistry **288,** 13156–13163.

Kramer DM, Johnson G, Kiirats O, Edwards GE. 2004. New fluorescence parameters for the determination of QA redox state and excitation energy fluxes. Photosynthesis Research **79,** 209.

Ladha JK, Tirol-Padre A, Reddy CK, Cassman KG, Verma S, Powlson DS, van Kessel C, de B Richter D, Chakraborty D, Pathak H. 2016. Global nitrogen budgets in cereals: A 50-year assessment for maize, rice, and wheat production systems. Scientific Reports **6,** 19355.

Laperche A, Brancourt-Hulmel M, Heumez E, Gardet O, Hanocq E, Devienne-Barret F, Le Gouis J. 2007. Using genotype × nitrogen interaction variables to evaluate the QTL involved in wheat tolerance to nitrogen constraints. Theoretical and Applied Genetics **115,** 399–415.

Li D, Tian M, Cai J, Jiang D, Cao W, Dai T. 2013. Effects of low nitrogen supply on relationships between photosynthesis and nitrogen status at different leaf position in wheat seedlings. Plant Growth Regulation **70,** 257–263.

Li H, Wang Y, Xiao J, Xu K. 2015. Reduced photosynthetic dark reaction triggered by ABA application increases intercellular CO_2 concentration, generates H_2O_2 and promotes closure of stomata in ginger leaves. Environmental and Experimental Botany **113,** 11–17.

Li Y, Gao Y, Xu X, Shen Q, Guo S. 2009. Light-saturated photosynthetic rate in high-nitrogen rice (*Oryza sativa* L.) leaves is related to chloroplastic CO_2 concentration. Journal of Experimental Botany **60,** 2351–2360.

Lian X, Xing Y, Yan H, Xu C, Li X, Zhang Q. 2005. QTLs for low nitrogen tolerance at seedling stage identified using a recombinant inbred line population derived from an elite rice hybrid. Theoretical and Applied Genetics **112,** 85–96.

Long SP, Bernacchi CJ. 2003. Gas exchange measurements, what can they tell us about the underlying limitations to photosynthesis? Procedures and sources of error. Journal of Experimental Botany **54,** 2393–2401.

Lu D, Lu F, Pan J, Cui Z, Zou C, Chen X, He M, Wang Z. 2015. The effects of cultivar and nitrogen management on wheat yield and nitrogen use efficiency in the North China Plain. Field Crops Research **171,** 157–164.

Mächler F, Oberson A, Grub A, Nösberger J. 1988. Regulation of photosynthesis in nitrogen deficient wheat seedlings. Plant Physiology **87,** 46–49.

Makino A. 2011. Photosynthesis, grain yield, and nitrogen utilization in rice and wheat. Plant Physiology **155,** 125–129.

Makino A, Mae T, Ohira K. 1986. Colorimetric measurement of protein stained with Coomassie Brilliant Blue R on sodium dodecyl sulfate-polyacrylamide gel electrophoresis by eluting with formamide. Agricultural and Biological Chemistry **50,** 1911–1912.

Miyake C, Yokota A. 2000. Determination of the rate of photoreduction of O_2 in the water-water cycle in watermelon leaves and enhancement of the rate by limitation of photosynthesis. Plant & Cell Physiology **41,** 335–343.

Nguyen NT, McInturf SA, Mendoza-Cózatl DG. 2016. Hydroponics: a versatile system to study nutrient allocation and plant responses to nutrient availability and exposure to toxic elements. Journal of Visualized Experiments, 54317.

Niyogi KK. 1999. Photoprotection revisited: genetic and molecular approaches. Annual Review of Plant Physiology and Plant Molecular Biology **50,** 333–359.

Richter J, Roelcke M. 2000. The N-cycle as determined by intensive agriculture – examples from central Europe and China. Nutrient Cycling in Agroecosystems **57,** 33–46.

Sage RF. 1990. A model describing the regulation of ribulose-1,5-bisphosphate carboxylase, electron transport, and triose phosphate use in response to light intensity and CO_2 in C_3 plants. Plant Physiology **94,** 1728–1734.

Sage RF, Pearcy RW. 1987. The nitrogen use efficiency of C_3 and C_4 plants: II. Leaf nitrogen effects on the gas exchange characteristics of *Chenopodium album* (L.) and *Amaranthus retroflexus* (L.). Plant Physiology **84,** 959–963.

Santarius KA, Heber U. 1965. Changes in the intracellular levels of ATP, ADP, AMP and P1 and regulatory function of the adenylate system in leaf cells during photosynthesis. Biochimica et Biophysica Acta **102,** 39–54.

Shangguan ZP, Shao MG, Dyckmans J. 2000. Effects of nitrogen nutrition and water deficit on net photosynthetic rate and chlorophyll fluorescence in winter wheat. Journal of Plant Physiology **156,** 46–51.

Sharwood RE, Sonawane BV, Ghannoum O, Whitney SM. 2016. Improved analysis of C_4 and C_3 photosynthesis via refined *in vitro* assays of their carbon fixation biochemistry. Journal of Experimental Botany **67,** 3137–3148.

Shi Z, Li D, Jing Q, Cai J, Jiang D, Cao W, Dai T. 2012. Effects of nitrogen applications on soil nitrogen balance and nitrogen utilization of winter wheat in a rice–wheat rotation. Field Crops Research **127,** 241–247.

Wang F, Gao J, Liu Y, Tian Z, Muhammad A, Zhang Y, Jiang D, Cao W, Dai T. 2016. Higher ammonium transamination capacity can alleviate glutamate inhibition on winter wheat (*Triticum aestivum* L.) root growth under high ammonium stress. PLoS One **11,** e0160997.

Wang K, Gao F, Ji Y, Liu Y, Dan Z, Yang P, Zhu Y, Li S. 2013. *ORFH79* impairs mitochondrial function via interaction with a subunit of electron transport chain complex III in Honglian cytoplasmic male sterile rice. New Phytologist **198,** 408–418.

Warren CR. 2004. The photosynthetic limitation posed by internal conductance to CO_2 movement is increased by nutrient supply. Journal of Experimental Botany **55,** 2313–2321.

Xing G, Zhu Z. 2000. An assessment of N loss from agricultural fields to the environment in China. Nutrient Cycling in Agroecosystems **57,** 67–73.

Yanagisawa S, Akiyama A, Kisaka H, Uchimiya H, Miwa T. 2004. Metabolic engineering with *Dof1* transcription factor in plants: Improved nitrogen assimilation and growth under low-nitrogen conditions. Proceedings of the National Academy of Sciences, USA **101,** 7833–7838.

Zhou YH, Yu JQ, Huang LF, Nogués S. 2004. The relationship between CO_2 assimilation, photosynthetic electron transport and water–water cycle in chill-exposed cucumber leaves under low light and subsequent recovery. Plant Cell and Environment **27,** 1503–1514.